A Novel Approach to Pile Foundations: Plant Root Architecture Application Using FEM

*Byong-Jeong Choi1) andJong-Hun Park2), Pil-Keun Park3), Sang-Hyeok Park4), Kyung-Tak Hong5)

1)Kyonggi University Department of Plant Architectural Engineering, San 94-6, Yiui-Dong, Yountong-Gu, Suwon-Si, Gyeonggi-Do, Republic of Korea 443-760*

1)bjchoi@kgu.ac.kr

2), 3), 4), 5)Gyeonggi Science High School, Suil-Ro 135, Jangan-Gu, SuwonSi, Republic of Korea

ABSTRACT

Plant roots typically have complex structures with specific architectural parameters characterizing the supporting effect of its root-soil system. This paper aims to propose a novel foundation design with a stronger supporting effect by applying plant root structure. A herring-bone pattern was selected and was applied to pile foundations for the common main axis, and mechanical properties were roughly set to match actual pile foundations. Various parameters were investigated and compared to understand how they influenced the supporting effect of the pile-soil system in whole. The supporting effect of the soil-pile structure was expressed via MIDAS FEA and results showed that root applied structures were significantly better in terms of the supporting effect and that the structural parameters should be adjusted for the contribution of soil in the system to be higher for better support.

---

1)Professor
2), 3), 4), 5)High School Student

I. Introduction

The significance of plant root architecture has been the tip of interest for the past few decades. This is because a considerable number of studies (Stokes 2009; Ip 2011; Preti 2009) have shown that plant roots play key roles in adhering and supporting grounds surrounding the plant. This is not a surprising issue considering that plants have had plant roots support themselves and the earth beneath them in various hazardous environments while undergoing evolution for a time far beyond human conception.

However, the purpose of plant roots is not only upholding the plant and reinforcing surrounding grounds, but also absorbing water and nutrients (Fitter 1987; Fitter 1991;Pierret 2007), storing nutrients, etc. This calls for a need in analyzing which part of the root structure attributes to the purpose most value is found, which in this paper is the stability of the plant. Previous studies on plant root systems show that parameters in the soil, such as water content(Fatahi 2007), soil internal friction angle and soil coefficients(Fourcaud 2008), and plant root parameters, such as the number of lateral roots(Crook 1996; Coutts 1983), asymmetry(Mickovski 2003), the degree between the roots and the main root(Dupuy 2005), various branching patterns(Khalilnejad) etc., join together to create the overall plant stabilization effect.

Although the effect of plant root architecture relating to its stability and the reinforcement of surrounding grounds has had been reviewed extensively, this has yet to be applied in the field of civil engineering. Nevertheless it is easily realized that the phenomenon of plant roots supporting itself is essentially the same as that of foundations. Foundations are in definition structures which transfer loads from their upper structure safely into the ground. Of these foundations, pile foundations and plant roots both have a single main axis as a common architectural parameter, but differ from the fact that piles are often drilled into bedrock while plant roots have branches and other complexities while floating above the bedrock. This is a crucial difference; plants have no choice but to make maximum use of soil friction in its roots' supporting phenomenon. Therefore, the approach to foundations by applying plant root architecture will need, first, recognizing the significance of the soil's supporting effect and second, understanding how the architectural parameters of the structure control the overall effect of support in both soil and foundation.

A rough mathematical model was proposed to get a glimpse on the complexity of the supporting forces of both pile and soil controlled by the structural parameters. However, the assumptions made for simplicity are far from the actual state. A careful consideration of the pile/soil system would need a more accurate model.

One powerful method in studying the phenomenon is using mathematical analysis tools such as the finite element method (FEM). Dupuy (2005) uses ABAQUS to analyze different root patterns and architectural parameters, also obtaining the contribution of such parameters to the anchorage of the roots. However, Dupuy did not seem to consider the correlation of the complex parameters of the architectural structure caused by various limits. This called for a need in categorizing the relations of the structural parameters under certain limit factors. Also, the material properties or the size of the model were considered for very small plant root structures, thus substituting these

values for those which match actual piles was also necessary. Loads were applied to model the process of pulling out the plant, whereas piles are pushed into the ground. In this paper, MIDAS FEM was used to simulate the strain on a pile/soil model under load conditions, thereby analyzing the various structural parameters' effect on the system's supporting effect.

Consequentially, a rough mathematical model was proposed to introduce the effects of the structural parameters to the supporting effect of the plant root architecture applied foundation. Using the FEM showed that applying plant root architecture ensured a bigger supporting effect compared to initial pile designs. Also structural parameters weighed on increasing the soil's supporting effect rather than the pile's supporting effect; therefore, we conclude that future pile designs should take the soil's supporting effect with deeper consideration.

II. Materials and methods

2.1 Nomenclature

α: Angle between a secondary segment and the main axis

r: Diameter of branch

l: Length of branch

dl: Total length of the branches

L: Length of the main axis

R: Diameter of main axis

n: Number of branches

μ: Friction coefficient

ρ: Density of soil

V_r: Volume of the pile model

D_b: Basal diameter of the pile model

Y_r: Young's modulus of pile

Y_s: Young's modulus of soil

s: Total displacement of pile model
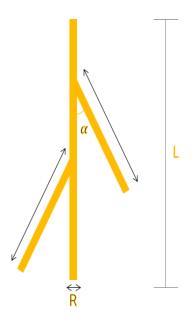
2.2 Parametric Modelling and Grouping of Plant Root System

Figure1Architectural Parameters of Root Pattern

This root pattern is determined by L, the length of the main axis, n, the number of secondary segments, α, the angle between a secondary segment and the main axis, and by the diameter of the main axis D_b and the total length of its secondary segments dlas in Fig. 1.

These parameters are given in Table 1. $L$was fixed as 30 m considering the fact that most bed rocks in the Korean Peninsula are found within that depth. αdetermines two sides of the supporting effect; how much it spreads out the load into the soil and the amount of soil beneath the branches. $\alpha \cong 0°$ will transmit the axial force best to the supporting grounds while a larger αwill have more soil beneath it, thus resulting in more spreading of the weight. However, for $\alpha > 90°$, the branches with axial force applied to the main axis will push the soil further away from the axis; therefore an angle exists between 0° and 90° where the supporting effect is maximized.

This pattern was divided into two separate groups by the limiting factor, *i.e.*diameter or volume. GroupD_b((a) of Fig. 2)'s main axis and secondary segments all have the same diameter constant as D_b(300mm) as of the reference model((c) of Fig. 3), while group V_r((b) of Fig. 2)'s models each has the total volume equal to the reference model. These limiting factors are important because of the fact that they control the relation between $n$and dl. In the case of group V_r, a longer $D_b$results in a decrease of the diameter in the main axis and the branches, thus weakening the pile itself. Also in both groups, a bigger $n$shortens the length of the branches, dl, thus reducing the amount of soil underneath. On the other hand, a bigger $n$also decreases the length of each section of the main axis, which results in increasing the maximum load it can tolerate.

Table 1Values of Paramaeters Selected

Parameters	Values			
L	30 m			
n	2		4	
α	45°	60°	75°	90°
dl	5 m		10 m	

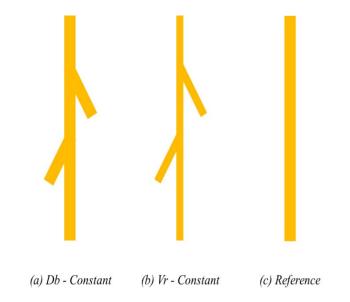(a) Db - Constant   (b) Vr - Constant   (c) Reference

Figure 2Restraint Conditions(a: radius constant, b: volume constant)

2.3 Rough Mathematical Model of Pile/Soil System's Support Effect

Most pile foundations only consider force from its strain, but it is possible, in the case of a cylindrical pile with length$L$and radius R, to get an extra force $F_{friction} = \pi\mu\rho g R L^2$. (g: gravitational acceleration) However, this is usually ignored, because of it being much smaller compared with $F_{strain} = \frac{Y_R \pi R^2}{L} s$.

The architectural structure of a root/soil system is the result of roots planting themselves into the ground using several growth strategies. Dupuy*etal.*analyzes three different growth patterns for the plant root system from previous studies. Considering the application to pile foundations, the herringbone-like root system, which has a fixed main axis, was selected to be analyzed.
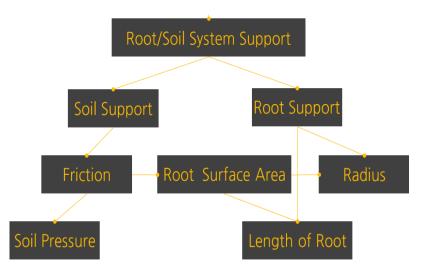
Figure 3 Diagram on Root/Soil Support's Relationship with its Subparameters

However, when the pile foundation is applied with plant root architecture, further forces other than just $F_{friction}$ are added. The following four forces are described in the Appendix.

$$F_{ss} = 2rY_S \, stan\alpha \left(\frac{n}{2} + \sum_{k=1}^{n} \frac{k}{n+1} \left(\frac{1}{cos\alpha} \frac{k}{n+1} \frac{L}{l} - 1\right) ln \left|1 - \frac{n+1}{k} \frac{l}{L} cos\alpha\right|\right) \tag{1}$$

$$f_{bf} = 2\pi\mu\rho gr \left(\frac{n}{2} Ll + \frac{n}{2} l^2 cos\alpha\right) cos\alpha + \frac{\mu n Y_R R^2 r}{(R^2 + brl)L} s(l^2 cos\alpha + \frac{\pi}{2} rlsin\alpha) cos\alpha \tag{2}$$

$$F_{bas} = Y_R \pi r^2 \left(\frac{1}{L} + \frac{1}{2l} cos^2\alpha\right)s \tag{3}$$

$$F_{brs} = \frac{1}{2} Y_R \pi ns(2l^2 tan^2\alpha - r^2)sin\alpha \tag{4}$$

$$F_{ss} : soil\ strain\ of\ force$$
$$f_{bf} : branch\ friction$$
$$F_{bas} : branch\ axial\ strain\ of\ froce$$
$$F_{brs} : branch\ rotational\ strain\ of\ froce$$

The total additional force F_{total} is the sum of these four forces. In our research, four structure variables (r, l, α, n) and two kinds of constraints (V_r, D_b) were selected. Changing a parameter has several effects due to the constraints, but it was thought that an optimized outcome would result with the right tinkering.

First, increasing α can increase F_{ss}, but also F_{bas} decreases. Similarly, increasing l can increase F_{ss}, but it causes a decrease in F_{brs}. Then which effect will be bigger? We can simply predict increasing F_{ss} will be better. Each forces (F_{ss}, F_{bas}, F_{brs}) has a

limit because too strong of a force will cause disruption of either pile or soil. Limits of these forces are similar to each other, but F_{bas} or F_{brs} is almost a thousand times bigger than F_{ss} because Y_R is 2000 ~ 4000 times bigger than Y_S. Let us name the total sum of forces regarding Y_R as F_R, and Y_S as F_S. It is simply expected that F_R will reach its yield limit more quickly than F_S, resulting in no more support. In this case, increasing α or l can increase the ratio between two forces $\frac{F_S}{F_R}$ and even if F_R is still at the limit as before, F_S becomes bigger, resulting in an increase of F_{total}. On the otherhand, if the ratio becomes too big, F_S will also reach its limit and when it passes it, F_{total} will start to decrease again.

Secondly, n increases the limit of F_R. It would seem like F_{total} would also increase in this case, but the yield of the branches must also be considered. More specifically, increasing n increases the limit of F_R of the main axis. Therefore, the main axis can sustain more weight, but the branches can't. This results in a decrease of F_{total}.

2.4 Mechanical Properties of Soil and Foundation

After defining the architectural parameters of the pile models, there was a need to assign various properties to the pile-soil system. In this study, two soil types were modelled which were considered as weak subsoil. Soil type 1 represented saturated soft clay while soil type 2 expressed loamy sand with low cohesion. The Mohr-Coulomb model was used as the yield criterion which explains the limit of soil failure. Other soil properties such as Young's modulus, Poisson's ratio etc. are given in Table 2 (Fourcaud 2008).

Table 2. Soil properties

Soil properties	Soil type 1	Soil type 2
Young's modulus (MPa)	5.0	10.0
Poisson's ratio	0.45	0.25
Cohesion c (kPa)	5.0	2.0
Friction angle (°)	2.0	40.0
Weight density (kNm-3)	1.0	1.5

The pile was set to be cylindrical, as in most piles, but defined as a concrete column for the sake of simplicity. Pile material was considered to be elastically linear, and the Von Mises model was applied to give the yield criterion of failure. Furthermore, the pile was modeled to have a Young's modulus of 20 GPa and a Poisson's ratio of 0.20. The average density of concrete at a limit load 50 MPa is known as 2,300 kg/m^3; therefore weight density was calculated as 2.26E-5 N/mm^3 as in Table 3.

Table 3. Pile properties

Pile properties	Pile
Young's modulus (MPa)	20,000.0
Poisson's ratio	0.20
Initial yield stress (MPa)	50.0
Weight density (kNm-3)	22.6

2.5 Boundary Conditions

The pile foundation was placed in the center of a $35m \times 35m$ square soil box. The thickness of the soil was adjusted to be equal to the diameter of the main axis in the pile for convenience in analyzing the system three-dimensionally with two-dimensional structural parameters. Boundary conditions of the soil box were defined to reproduce the surrounding infinite earth; only upward and downward translation was possible for the two lateral faces. The underside of the soil box and pile model were both fixed to model the bedrock and the pile driven into the bedrock.

The pressure of the soil p was linearly increased from the top to the bottom with gravity and a pressure of 1kPa was applied to the top surface of the soil to express the atmospheric pressure. These conditions are expressed in Fig. 4.
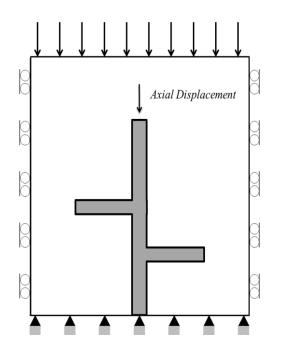

Figure 4. Boundary Conditions for Soil/Pile Model

2.6 Numerical investigation

Numerical investigation was performed using the finite element analysis program MIDAS FEA, which was provided by the steel structure laboratory in Gyeonggi University.

2.6.1 Mesh Generation

To conduct the finite element analysis, models were needed to be divided into a number of small units called meshes. The mesh size for all pile models remained constant as the radius of the main axis. For the soil model, the size of the meshes was set as 6 m. Both models' meshes were created using the auto mesh function.

2.6.2 Load Conditions

To observe the strain of the pile foundation, compression force was used in this study; axial load was applied to the top surface of the main axis in the pile model. Though the limit load of concrete is already known to be around 50 MPa, various boundary conditions controlling the interface between the soil and the pile makes it difficult to estimate the maximum load the pile-soil system can withhold. Therefore, the initial axial load was set as 0.01% of 50 MPa, and increased until the model reached failure.

2.7 Stress-Strain Measurement

We defined the nodes as shown in Fig. 5. The nodes in the reference model were selected to have the same depth and the same soil pressure as in the pile models. Displacement, change of the node's position from before applying the load to after, was compared for every node at certain loads, enabling to pinpoint the better structure.
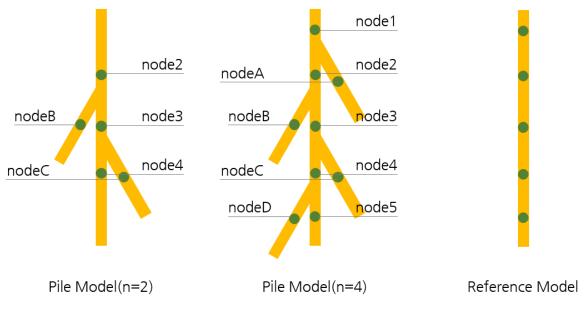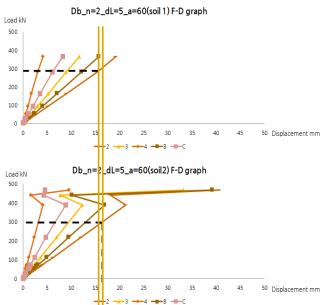

Figure 5. Naming of nodes in Model

2.8 Output of the Model

Concrete is a material in which the yield criterion is controlled by the initial cracks in the structure. After a crack is created, the foundation was thought as no longer able to support the load above. Force-displacement relationship curves(p-δ) of the model under load conditions were acquired from the FEM simulations. p-δrelationship curves are divided into two discrete sections in which the first section has a linear correlation until a certain point, and a second section with sudden non-linear bends after that point. This point was analyzed as the point of fracture in the structure. Most models were found to be under higher pressure than the reference model before fracturing; therefore the δvalue on the $p$value of the reference model's point of fracture was used to compare which models had the better structure in terms of stability.

The results of the p-δrelationship curves in all models showed that the highest node had the earliest fractures in the structure. Therefore, these nodes were selected, *i.e.* node 1 in n=4 models and node 2 in n=2 models, to be compared with the reference model.
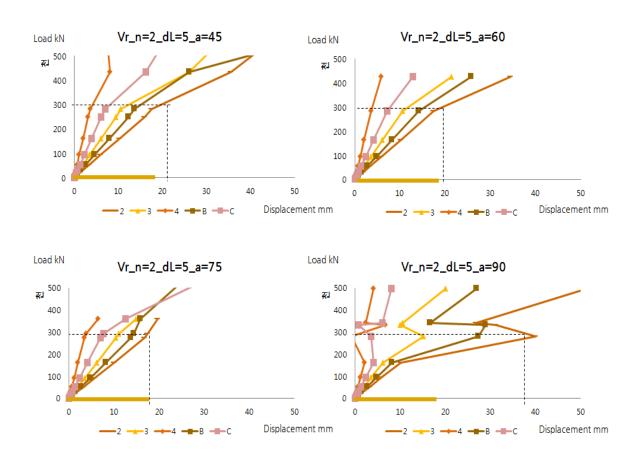
III. Results

The analysis using finite element method showed how the parameters defined in the methodology affected the supportingeffect of the pile-soil system.

3.1Influence of Soil

Figure 6 Influence of Soil (top: clay, bottom: sand)

Soil type 1(saturated clay) and soil type 2(loamy sand) were considered in this research. The yellow lines in Fig. 6 show the difference of the minimum displacement in the models. The model in soil type 1 showed better results.

3.2 Influence of angle, α

Figure 7 Influence of Angle (upper left: 45°, upper right: 60°, lower left: 75°, lower right: 90°)

The models in the conditions of $n = 2$, and $dl = 5$ in group V_r were compared by varying α from 45 degrees to 90 degrees. As shown in Fig. 7, maximum displacement was compared at the load of 300kN. The yellow bars show the displacement at the model with $\alpha = 75$, thus $\alpha = 75$ had the best structure under such conditions.
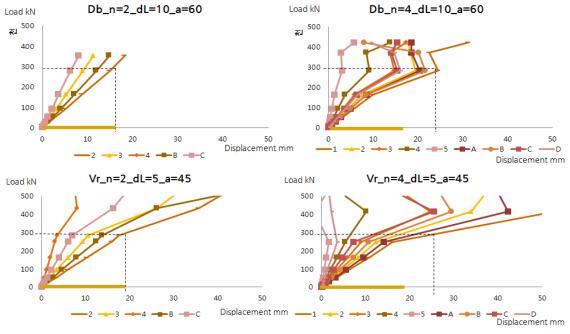
3.3 Influence of number of branches, n

Figure 8 Influence of number of branches

The models with conditions $dl = 10$, $\alpha = 60$ in group D_b and $dl = 5$, $\alpha = 45$ in group V_r were compared with n varied as 2 or 4. Fig. 8 indicates n=2 to have a smaller displacement than of n=4 in both constraint conditions.

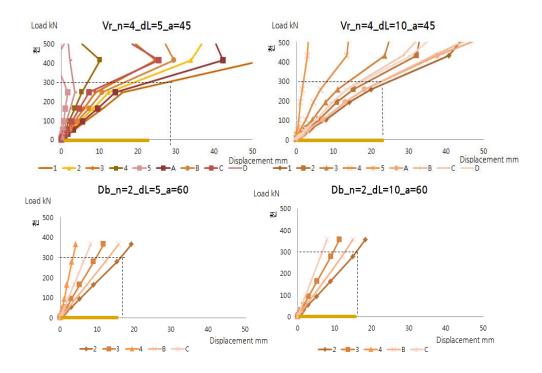3.4 Influence of total root length dl

3730

Figure 9 Influence of Total Root Length

The models with conditions $n = 4$, $\alpha = 60$ in group D_b (upper left and right of Fig. 9) and $n = 4$, $\alpha = 45$ in group V_r (lower left and right of Fig. 9) were compared with dl varied as 5 or 10. As shown in Fig. 9 as the yellow bars, the models with $dl = 10$ had smaller displacements than models with $dl = 5$, which implied that increasing dl under these conditions created better structures.

IV. Discussion

4.1 Influence of Parameters to Supporting Effect of Soil/Pile System

4.1.1 Support by Soil

Similar curves resulted in both types of soil. However the small difference must be recognized, because of the usage of several piles in the support of a building. Different results showed in different soils.

4.1.2 Support by α

Similar curves resulted in both groups V_s and D_b. Maximum stress yields differed slightly with the change in α. The optimum effect was found when α was $75°$ which matched the expectations of α having an optimum value between 0 and 90 degrees in section 2.2.

4.1.3 Support by n

Similar curves resulted in both groups V_s and D_b. Maximum stress yields differed slightly with the change in n. The optimum effect, which was when $n = 2$, indicates that the amount of soil under the branches has a bigger effect on the supporting effect of piles than the decrease of section length.

4.1.4 Support by dl

Group D_b's results showing $dl = 10$ as the optimum value was not surprising considering that the limiting factor of D_b has no negative effect, but group V_r also had the same results. This indicates that the diameter decrease had a smaller effect compared to the increase in the branches' length.

4.2 Overall Influence of Parameters

Structural parameters α, dl, n all had their values weighed on increasing the soil's effect of support rather than increasing the pile's support.

4.3 Conclusions

Previous research showed that plant root architecture had a significant effect on adhering grounds and supporting itself. Yet, no papers applying plant root architecture to civil engineering were found. Hereupon, the supporting effect of the pile foundation was found to be influenced by the architecture of the pile and boundary conditions between the pile and soil. Also, the limiting factors D_b and V_r created an optimum structure, because of its weighing various subparameters controlling the supporting effect against each other. Of these the amount of soil under the branches was found to be most important.

Furthermore, few papers discuss the conditions of the pile foundation actually inside the ground. The pile-soil models described are important simplifications of the situation itself and in many ways idealistic, but since there are no other ways available for analyzing in-situ piles, future studies focusing on foundations might benefit from the modelling approach described in this paper.

4.4 Further Research

The possibility of applying plant root architecture to pile foundations was found to be promising, but still lacks a construction method, and had considered various factors due to simplification reasons. Also, the analysis was based on two-dimensional structural parameters, but this should be analyzed under three-dimensional parameters to match reality. Finally these parameters should also be analyzed under horizontal and/or vertical oscillation forces for research on foundation stability against earthquakes.

V. References

Coutts, M. P. (1983), "Root architecture and tree stability", *Plant and Soil,* Vol. 71, 171-188
Crook, M.J., andEnnos, A.R. (1996), "The anchorage mechanics of deep rooted larch, Larixeuropea x L japonica", *Journal of Experimental Botany*, Vol. 47(303), 1509-1517

Dupuy, L., Fourcaud, T., Lac, P. and Stokes, A. (2007), "A Generic 3D Finite Element Model of Tree Root Anchorage Integrating Soil Mechanics and Real Root System Architecture",*Am. J. Bot.,*Vol. *94(9),* 1506–1514.

Dupuy, L., Fourcaud, T., and Stokes, A. (2005), "A Numerical Investigation into Factors Affecting the Anchorage of Roots in Tension", *European Journal of Soil Science,*Vol.56, 319–327.

Fatahi, B., Indraratna, B., andKhabbaz, H., "Analyzing Soft Ground Improvement Caused by Tree Root Suction", *American Society of Civil Engineers,* pp. 1-10.

Fitter,A. H., Stickland, T. R., Harvey, M. L. and Wilson, G. W. (1991), "Architectural Analysis of Plant Root Systems. 1. Architectural Correlates of Exploitation Efficiency", *New Phytologist*, Vol. 118(3), 375-382

Fitter,A. H. (1987), "An Architectural Approach to the Comparative Ecology of Plant Root Systems", *New Phytologist*, Vol. 106(1), pp. 61-77.

Khalilnejad, A., Ali, F. H., Hashim, R., and Osman, N. "Finite element simulation for the impact of Root Morphology on pulling-out process"

Mickovski, S. B., andEnnos, A. R. (2003), "Anchorage and Asymmetry in the Root System of Pinuspeuce", *Silva Fennica,* Vol.37(2), 161–173.

Pierret, A., Doussan, C., Capowiez, Y., Bastardie, F., andPagès, L. (2007), "Root Functional Architecture: A Framework for Modeling the Interplay between Roots and Soil", *Vadose Zone*, Vol. 6(2), 269-281.

Preti F., and Giadrossich, F. (2009), "Root reinforcement and slope bioengineering stabilization by Spanish Broom (SpartiumjunceumL.)", *Hydrol. Earth Syst. Sci. Discuss.,* Vol. 6, 3993-4033

Stokes, A., Atger, C., Bengough, A. G., Fourcaud, T. and Sidle. R. C.(2009), "Desirable plant root traits for protecting natural and engineered slopes against landslides", *Plant and Soil*, 324(1), 1–30

Wu, T. H., Beal.P. E., and Lan, C. (1988) "In-Situ Shear Test of Soil-Root Systems", Journal of Geotechnical Engineering, Vol. 114(12), pp. 1376-1394

VI. Appendix
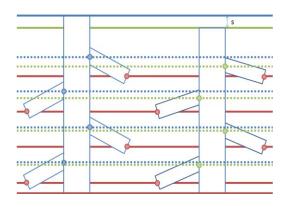
Calculation of Forces

Figure 10. Assumption of Pile's Tendency Under Strain

The tip of the branches (red points) were thought to be fixed. When force is applied, the blue points in Fig. 10 were thought to move to the green points.
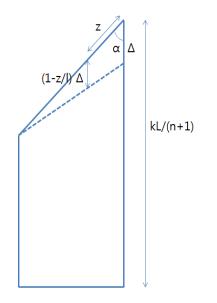
5.1 $F_{soil\ strain}$

Figure 11 Diagram for Calculation of F_{ss}

Let z be the length from the point of intersection of a branch and the main axis as in Fig. 11. Strain at z is $(1 - \frac{z}{l})\Delta$, and height branch is $\frac{k}{l+1}L$, so height of soil column before strain is $\frac{k}{l+1}L - z\cos\alpha$. Cross section of this soil column is $2r\sin\alpha dz$, so force from soil under kth branch is $\int_0^l Y_s \frac{(1-\frac{z}{l})\frac{k}{n+1}S}{\frac{k}{n+1}L - z\cos\alpha} 2r\sin\alpha dz$. With some calculation, the following equation can be obtained.

$$F_{ss} = 2rY_S s\tan\alpha\left(\frac{n}{2} + \sum_{k=1}^{n} \frac{k}{n+1}\left(\frac{1}{\cos\alpha}\frac{k}{n+1}\frac{L}{l} - 1\right)ln\left|1 - \frac{n+1}{k}\frac{l}{L}\cos\alpha\right|\right) \tag{1}$$
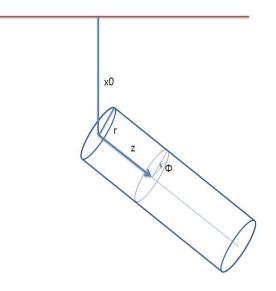
3734

5.2 $F_{branch\ friction}$

Figure 12Diagram for Calculation off_{bf}

Depth of an infinitesimal soil element $x = x_0 + z\cos\alpha - r\sin\alpha\cos\Phi$ as in Fig. 12. Soil pressure $P = \rho g x$, thus differential force $dF = \mu P da$ (da : differential cross section). $da = rd\Phi dz$, so the total force is $\mu \int P da = \mu \rho g r \int_0^l \int_0^{2\pi} (x_0 + z\cos\alpha - r\sin\alpha\cos\phi) d\phi dz$. With some calculation, the value $2\pi\mu gr(x_0 l + \frac{1}{2}l^2\cos\alpha)$ is obtained, but its z directional components is $2\pi\mu gr(x_0 l + \frac{1}{2}l^2\cos\alpha)\cos\alpha$.

When an additional force Fpushes down, there will be additional pressure at the bottom half of each branches. (Top half doesn't get additional pressure because the reason of the pressure is the structure pushing the soil downward because of F) The additional pressure is $\frac{1}{R^2+nrl}\frac{F}{\pi}$, so additional force is $\mu \int P_{add}(-\cos\phi)da = -\frac{\mu}{R^2+nrl}\frac{F}{\pi}r\int_0^l \int_{\frac{\pi}{2}}^{\frac{3}{2}\pi}(z\cos\alpha\cos\phi - r\sin\alpha\cos^2\phi)d\phi dz$ (the minus sign added because at the range of $\frac{\pi}{2} \le \phi \le \frac{3}{2}\pi$, $\cos\phi$ is negative.) With some calculation, the value $\frac{\mu}{R^2+nrl}\frac{F}{\pi}r(l^2\cos\alpha + \frac{\pi}{2}rl\sin\alpha)$ is obtained. Its z directional components is $\frac{\mu}{R^2+nrl}\frac{F}{\pi}r(l^2\cos\alpha + \frac{\pi}{2}rl\sin\alpha)\cos\alpha$. But $x_0 = \frac{k}{n+1}L$, and $F = Y_R\pi R^2\frac{s}{L}$, so the total force becomes $\sum_{k=1}^n (2\pi\mu gr\left(\frac{k}{n+1}Ll + \frac{1}{2}l^2\cos\alpha\right)\cos\alpha + \frac{\mu Y_R R^2 r}{(R^2+nrl)L}s(l^2\cos\alpha + \frac{\pi}{2}rl\sin\alpha)\cos\alpha)$.

With some calculation, the following equation is obtained.

$$f_{bf} = 2\pi\mu\rho g r \frac{n}{2}(Ll + l^2 cos\alpha)cos\alpha + \frac{\mu n Y_R R^2 r s}{(R^2 + nrl)L}\left(l^2 cos\alpha + \frac{\pi}{2}rlsin\alpha\right)cos\alpha \qquad (2)$$
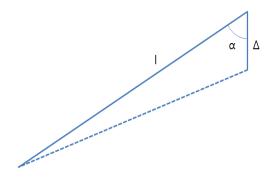
5.3 $F_{branch\ axial\ strain}$

Figure 13 Diagram for Calculation of F_{bas}

The strain of the branch (dotted line) of initial length l, angle α, and strain (of middle pile) Δ is $l - \sqrt{l^2 + \Delta^2 - 2l\Delta cos\alpha} \approx \Delta cos\alpha$. ($l \gg \Delta$). (See Fig. 13)

The force from the strain is $Y_R \pi r^2 \frac{\Delta cos\alpha}{l}$, and $\Delta = \frac{k}{n+1}s$ (k = 1, 2, $\cdots$, n), so total force

from strain is $Y_R(\pi R^2 \frac{s}{L} + \pi r^2 \frac{\sum_{k=1}^{n}\frac{k}{n+1}scos\alpha}{l})$. Its z directional component is $Y_R(\pi R^2 \frac{s}{L} +$

$\pi r^2 \frac{\sum_{k=1}^{n}\frac{k}{n+1}scos\alpha}{l})cos\alpha$. With some calculation the following equation is obtained.

$$F_{bas} = Y_R \pi r^2 (\frac{1}{L} + \frac{1}{2l}cos^2\alpha)s \qquad (3)$$

5.4 $F_{branch\ rotational\ strain}$
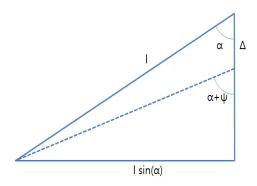

Figure 14 Diagram for Calculation of F_{brs}

There is a small change of angle ψ because of the compression. As in Fig. 14, $\frac{l\sin\alpha}{\tan\alpha} = \frac{l\sin\alpha}{\tan(\alpha+\psi)} + \Delta$. So, $\frac{l\sin\alpha}{\cos\alpha - \Delta} = \tan(\alpha+\psi) \approx \tan\alpha + \tan\psi \approx \tan\alpha + \psi$ and $\psi = \frac{\Delta\tan\alpha}{l\cos\alpha - \Delta} \approx \frac{\Delta}{l}\sin\alpha$.
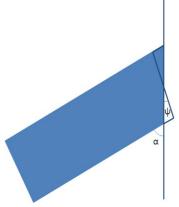

Figure 15

The differential cross section is $2r^2\sin\phi d\phi$, so total torque from strain is $\int_0^\pi Y_R \frac{2r^2\sin^2\phi d\phi}{l+r\frac{\cos\phi}{\tan\phi}} (r\frac{\cos\phi}{\tan\alpha} - r\frac{\cos\phi}{\tan(\alpha+\psi)})r\cos\phi$. But $r\frac{\cos\phi}{\tan\alpha} - r\frac{\cos\phi}{\tan(\alpha+\psi)} \approx r\frac{\cos\phi}{\tan^2\alpha}\psi$, so the result becomes $Y_R l\pi\psi(2l^2\tan^2\alpha - r^2)$. The end of the branch is fixed, so force per length (f) is proportional to $l - z$. Let $f = \kappa(l - z)$, then $\tau = \int_0^l \kappa(l - z)dz$ so $\kappa = \frac{6\tau}{l^3}$. So the total force from each branch becomes $\int_0^l \kappa(l-z)dz = \frac{3\tau}{l} = Y_R\pi\Delta(2l^2\tan^2\alpha - r^2)\sin\alpha$. But $\Delta = \frac{k}{n+1}s(k = 1,2,\cdots,n)$, so the total force becomes $\sum_{k=1}^n Y_R\pi\frac{k}{n+1}s(2l^2\tan^2\alpha - r^2)\sin\alpha$. After some calculation, we can get the equation.

$$F_{brs} = \frac{1}{2}Y_R\pi ns(2l^2\tan^2\alpha - r^2)\sin\alpha \cdots \tag{4}$$